第42卷 第2期
2013年2月

人 工 晶 体 学 报
JOURNAL OF SYNTHETIC CRYSTALS

Vol. 42 No. 2
February, 2013

Synthesis and Characterization of Nanocrystalline $La_{0.67}Ca_{0.33}MnO_3$ Powder by a Simple Sol-gel Method

Mya Theingi[1,2], *MA Ji*[1], *ZHANG Hui*[1], *WANG Wen-zhang*[1], *YI Jian-hong*[1], *CHEN Qing-ming*[1]

(1. Faculty of Materials Science and Engineering, Kunming University of Science and Technology, Kunming 650093 China;
2. Department of Chemistry, University of Yangon, Yangon 11181, Myanmar)

(*Received* 2 *May* 2012, *accepted* 2 *July* 2012)

Abstract: Nanocrystalline powders of manganite perovskite $La_{0.67}Ca_{0.33}MnO_3$ were prepared by a simple sol-gel method at relatively low temperature. Single nanosized perovskite phase can be produced when the dried gel was calcined at the temperature as low as 500 ℃ without any intermediate step that was confirmed by X-ray diffraction. The prepared calcined powders are nanocrystalline up to 900 ℃ (particle size ranging from 30 nm to 80 nm). However the crystalline particles are significantly grown (micron-sized grain) after the powders had been pressed into pellets and sintered at 1100 ℃. The morphology of bulk polycrystalline target and their electrical transport measurements were performed by using scanning electron microscope (SEM) and a conventional four probe technique, respectively. Remarkably sharp peaks of the resistivity vs. temperature (ρ-T) curves with insulator-metal transition temperature T_{IM} (around 270 K) can be observed.

Key words: sol-gel method; nanocrystalline powders; manganite perovskite; $La_{0.67}Ca_{0.33}MnO_3$

CLC number: **Document code**: A **Article ID**: 1000-985X(2013)02-000-00

一种简便的溶胶-凝胶法制备的 $La_{0.67}Ca_{0.33}MnO_3$ 纳米晶粉末的结构与性能

Mya Theingi[1,2], 马 吉[1], 张 辉[1], 王文章[1], 易健宏[1], 陈清明[1]

(1. 昆明理工大学材料科学与工程学院, 昆明 650093; 2. 仰光大学化学学院, 仰光 11181, 缅甸)

摘要: 采用一种比较简单的溶胶-凝胶法在相对较低的温度下制备了钙钛矿锰氧化物 $La_{0.67}Ca_{0.33}MnO_3$ 纳米粉末。XRD结果显示干凝胶直接在500 ℃下煅烧即可得到单一钙钛矿相, 而无需任何其他中间步骤。当煅烧温度从500 ℃上升到900 ℃时, 纳米晶的尺寸相应的从30纳米长大到80纳米左右。分别采用扫描电镜和传统的四探针法表征了多晶靶材的表面形貌和电输运性能, 观察到了电阻率-温度(ρ-T)曲线上绝缘体-金属转变温度 T_{IM} 附近(270 K左右)非常陡的电阻率变化。

Received date: 2012-05-02; **accepted date**: 2012-0-0

Foundation item: the project supported by National Natural Science Foundation of China (50902062) and the Scientific Research Foundation for the Returned Overseas Chinese Scholars, State Education Ministry

Biography: Mya Theingi (1975-), Female, from Myanmar, Ph. D. E-mail: mya. tt. chem@ gmail. com

Corresponding anthor: Chen Qing-ming, Professor(Ph. D.), E-mail: chqm99@ yahoo. com

关键词:溶胶-凝胶法;纳米晶粉末;钙钛矿锰氧化物;$La_{0.67}Ca_{0.33}MnO_3$

1 Introduction

The discovery of manganese-based perovskite materials, called the colossal magnetoresistive (CMR) materials, has generated a considerable interest because of their various electronic, magnetic and structural properties and potential applications[1-3]. Soon after the discovery of the properties of CMR materials, there has been considerable experimental and theoretical interest in perovskite manganese oxides of the type $R_{1-x}A_xMnO_3$, where R and A are rare earth and alkaline-earth elements, respectively. These systems are known to exhibit a number of unusual and interesting electronic properties, among which the insulator-metal transition and the CMR effect are probably the most dramatic one. The parent compound $RMnO_3$ which is an antiferromagnetic, when doped with divalent ions (A), can be driven into a metallic ferromagnetic state at low temperature by a process known as 'double exchange (DE)' mechanism occurring between Mn^{3+} and Mn^{4+} proposed by Zener[4]. The high temperature's paramagnetic insulating behavior was caused by so called Jahn-Teller effect, which is competed with double exchange[5]. The bulk polycrystalline samples of perovskite-type lanthanum manganese oxides are usually prepared by the conventional solid state reaction, where higher temperature, longer sintering time and several times of intermediate grinding are necessary to obtain a homogenous composition desired compound[6]. Until now, a large number of methods such as co-precipitation[7], sol-gel[8], hydrothermal[9], polyvinyl alcohol (PVA) route[10] etc. are used to synthesize nanocrystalline particles with desired size and narrow distribution. The physical properties of these samples are usually dependent on their preparation routes[11]. Furthermore, the nanostructure material has been predicted to provide some new features in magnetic properties compared to bulk materials[12,13]. The sol-gel method has some potential advantages compared to other methods. The most evident advantage of the sol-gel method is that reagents are mixed in atomic level, which may increase the reaction rate and decrease the synthesis temperature, and can be synthesis more homogeneous samples[14-17]. In the present work, we report on synthesis of single perovskite phase nanosized $La_{0.67}Ca_{0.33}MnO_3$ (LCMO) by a simple and one-step sol-gel method at calcined temperature as low as 500°. The investigations on the structure and physical properties of the resulting LCMO reveal that the polycrystalline ceramic have high crystalline and single phase.

2 Experimental

$La(NO_3)_3 \cdot nH_2O$, $Ca(NO_3)_2 \cdot 4H_2O$, $Mn(NO_3)_2$ (Grade: AR) were used as raw materials to prepare $La_{0.67}Ca_{0.33}MnO_3$ powder. Firstly, the desired molar ratios La: Ca: Mn of 2: 1: 3 were dissolved in deionized water by stirring at room temperature. The citric acid solution, used as a chelating agent, was added to this solution. Molar ratio between the citric acid and the metal ions was 2: 1. Subsequently 5 mL of ethylene glycol, used as a gelification agent, was also added to the mixture solution. The resulting solution was directly heated at 80 ℃ under continuous stirring. After being heated for about 6 h, the solution became highly viscous, the transparent gel was formed. Finally, the xerogel was obtained after the gel was dried completely at an oven at 120 ℃ for 12h to obtain a beige solid which upon calcinations in air at different temperature (500-900 ℃) for 16 h. The resulting calcined powders were pressed into pellets and sintered at 1100 ℃ for 16 h to get bulk polycrystalline ceramic targets. In order to study thermal decomposition mechanism of the dried gel powders, thermogravimetry and differential scanning calorimetry (TG-DSC) analyses were carried out with a STA 449 *F*3 analyzer. The samples were heated in air and heating rate was 10 ℃/min. X-ray diffraction (XRD) measurement was performed on a (BDX3200) diffractometer with Cu K_α radiation ($\lambda_{K\alpha 1} = 0.154056$ nm) to investigate the phase identification and structural

analysis of the samples. Scanning electron microscope (SEM) with XL30ESEM-TMP (Philips, Holland) was performed to investigate the morphology of the synthesized powders and pelletized polycrystalline ceramics. To investigate the electrical transport properties of pelletized polycrystalline ceramic, the temperature dependence of resistivity (ρ-T) was performed by using conventional four-probe method.

3 Results and discussion

TG-DSC results of the dry xerogel LCMO powders are shown in Fig. 1. Two slight and a sharp endothermic peaks were observed in the DSC trace. The slight endothermic peak appeared at around 100-160 ℃ accompanied with 15% weight loss in TG trace was due to loss of water from the xerogel precursor and low boiling point organic species. The slight broad endothermic peak between 170 ℃ and 350 ℃ accompanied with ~30 % weight loss was due to the decomposition of related coordination species[18]. The sharp endothermic peak between 350 ℃ and 450 ℃ is nearly vertical in the DSC trace accompanied with ~30% weight loss is caused by the decomposition of residual organic compounds of the precursor[19]. Above 450 ℃ there are no found evident heat absorb or release process on DSC trace, it has been revealed that this is due to the formation of perovskite phase and crystallization process occur at that temperature period. By XRD analysis, it can be seen small and broad diffraction peaks for the 500 ℃ calcined powder, but no visible peak for 400 ℃ powder, which may because the initial particle size are too small to be detected by XRD. After 650 ℃, there is observed gradually increased exothermic heat flow on DSC trace accompanied with no evidence weight loss in TG trace that may be caused by the growing grain size process. This process was also confirmed by X-ray diffraction analysis.

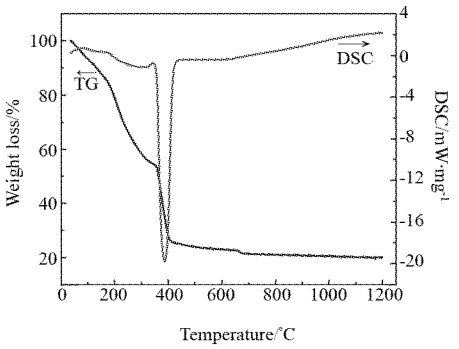

Fig. 1　TG-DSC traces for xerogel LCMO

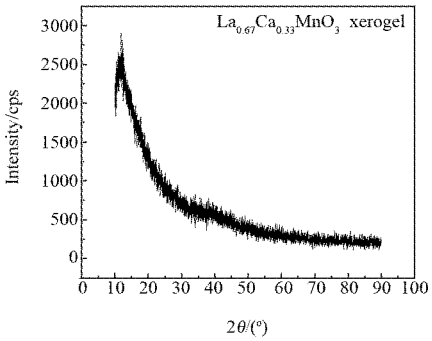

Fig. 2　XRD pattern of xerogel LCMO

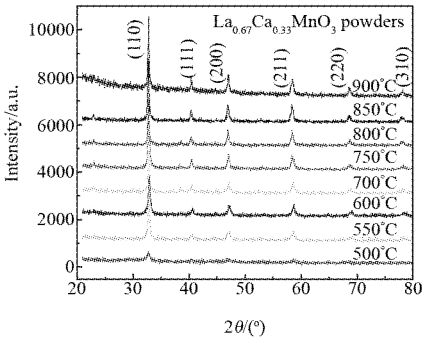

Fig. 3　XRD patterns of LCMO powders at different temperatures for 16 h

LCMO xerogel and powders, obtained from calcined at different temperatures, characterized by XRD (using diffraction angles of 2θ between 20° and 80°), are also shown in Fig. 2 and Fig. 3, respectively. It cannot be seen any diffraction peak in the dried xerogel XRD pattern, which indicates that the gel is mainly amorphous. Fig. 3 shows diffraction peaks of LCMO powders calcined at different temperatures. All samples are single phase with no detectable secondary phases. The average crystallite size of the synthesized powders was estimated from the full width at half-maximum (FWHM) (110) peak via the classical Scherrer formula[20]:

$$D = \frac{0.89\lambda}{\beta\cos\theta}$$

Where D is the crystallite size in nm, λ is the radiation wavelength (0.154056 nm for Cu K_α), β is the difference of the FWHM of the peak between the sample and the standard SiO_2 used to calibrate the intrinsic width associated to the instruments, and θ is the diffraction peak angle. The graph of the calculated crystallitic sizes vs. their calcined temperatures was illustrated by Fig. 4. It shows that the crystallite size increases obviously with the calcined temperature shifting from 500 ℃ to 900 ℃. According to TG-DSC and XRD analysis, we have successfully synthesized single-phase nanosized LCMO at relatively low temperature without any intermediate step. This may be due to the salts in the prepared precursor were uniformly distributed and were not isolated[21].

The SEM micrographs of LCMO powders calcined at 500 ℃ and 900 ℃ were illustrated by Fig. 5(a) and (b). The homogeneous tiny crystalline aggregates can be seen in the micrograph with the heat treatment of 500 ℃. At higher calcined temperature (900 ℃) agglomerates of nanocrystalline LCMO particles (~100 nm) can be seen, which is larger than XRD calculation results in Fig. 4. As can be seen from the graph, the higher calcined temperatures, the larger crystallitic particle size, and the more apparent the agglomeration process. For sintering high density ceramic, the crystallite particles are agglomerated in to grains and the grain boundaries are appeared, as can be seen in Fig. 6(b). So, the high density ceramic target is preferable to prepare thin films.

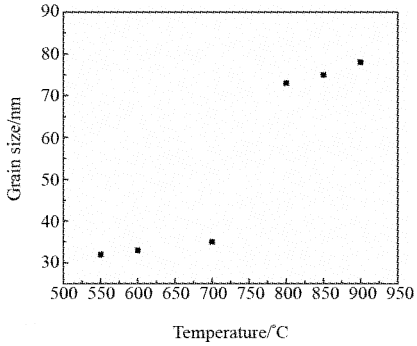

Fig. 4 Temperature dependence of the crystallite size of $La_{0.67}Ca_{0.33}MnO_3$ powder measured at different temperatures

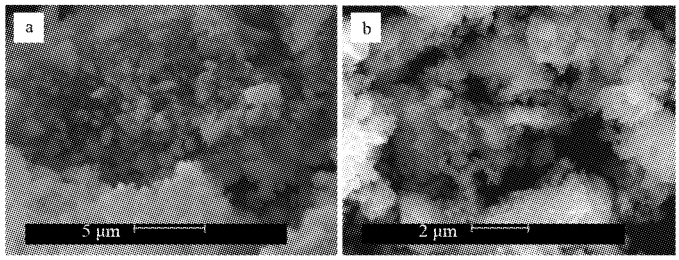

Fig. 5 SEM micrographs of LCMO nanocrystalline particles calcined at (a)500 ℃; (b)900 ℃ for 16 h

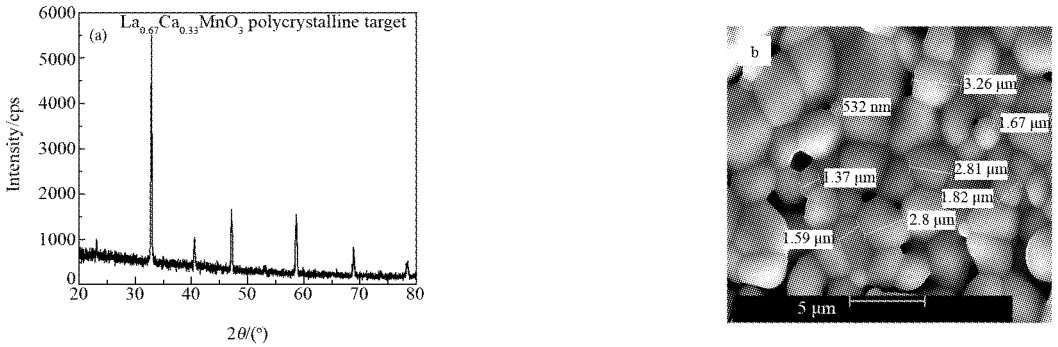

Fig. 6 (a) X-ray diffraction pattern and (b) SEM micrograph of LCMO bulk polycrystalline target sintered at 1100 ℃ of the powder calcined at 500 ℃

X-ray diffraction pattern and SEM micrograph of LCMO bulk polycrystalline target sintered at 1100 ℃ of the

powder calcined at 500 ℃ was shown in Fig. 6 (a) and (b), respectively. It can be seen that the prepared bulk sample has single phase and higher crystalline quality than the powders. As a consequence of the high sintering temperature heat treatment, crystallinity and agglomeration process increased.

The temperature dependence of resistivity was measured by four probe technique in the temperature range ~ 100-300 K. Fig. 7 shows the metal-insulator transition curves of bulk polycrystalline LCMO targets after pelletizing and sintering at 1100 ℃ of the powders calcined at different temperatures. The insulator-metal transition temperature TIM can be observed in all bulk targets. Due to disorders and local strain in the grain boundary region, the resistivity peak became broader and the temperature of the insulator metal transition, TIM, shifted to lower values[22]. In our results all the peak values of the metal-insulator transition curves are remarkably sharp and at the typical temperature around 270 K, which demonstrate that the prepared powders have been completely composited to the single phase LCMO.

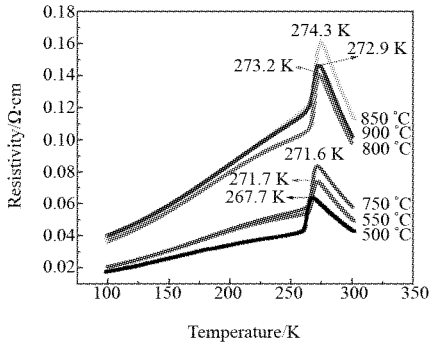

Fig. 7　Temperature dependence of the resistivity of buck polycrystalline LCMO targets sintered at 1100 ℃ from the powders of different calcined temperatures

4　Conclusion

Nanocrystalline LCMO powders have been synthesized by a simple one-step sol-gel method. The major advantage of this method is that even at relatively low calcined temperature (~ 500 ℃) xerogel precursors are directly transformed into a single perovskite phase without intermediate step. The bulk polycrystalline targets (sintered at 1100 ℃) display remarkably sharp insulator-metal transition behavior. These results are comparable to those for LCMO powders and bulk samples synthesized by solid state and co-precipitation methods.

参 考 文 献

[1] Schiffer P, Ramirez A P, Bao W, et al. Low Temperature Magnetoresistance and the Magnetic Phase Diagram of $La_{1-x}Ca_xMnO_3$[J]. *Phys. Rev. Lett.*, 1995, **75**: 3336.

[2] Tan G T, Dai S Y, Duan P, et al. Structural Electric and Magnetic Properties of the Electron-doped Manganese Oxide: $La_{1-x}Te_xMnO_3$ ($x = 0.1$, 0.15)[J]. *J. Appl. Phys.*, 2003, **93**: 5480.

[3] Roy S, Ali N. Charge Transport and Colossal Magnetoresistance Phenomenon in $La_{1-x}Zr_xMnO_3$[J]. *J. Appl. Phys.*, 2001, **89**: 7425.

[4] Zener C. Interaction Between the D-shells in the Transition Metals Ⅱ Ferromagnetic Compounds of Manganese with Perovskite Structure[J]. *Phys. Rev.*, 1951, **82**: 403.

[5] Millis A J. Lattice Effects in Magnetoresistive Manganese Perovskites[J]. *Nature, London*, 1998, **392**: 147.

[6] Deng H, Yang C P, Zhou Z H, et al. Electroresistance Effect in $La_{1-x}Ca_xMnO_3$ ($0 < x < 1$) Ceramics[J]. *J. Phys. Chem. Solids*, 2010, **71**: 660.

[7] Maurin, Barboux P, Lassailly Y, et al. La (Sr, Pb) MnO_3, Thin Films Through Solution Techniques[J]. *Chem. Mater.*, 1998, **10**: 1727.

[8] Li Y Y, Yao S S, Xue LY, et al. Sol-gel Combustion Synthesis of Nanocrystalline $LaMnO_3$ Powders and Photocatalystic Properties[J]. *J. Mater. Sci.*, 2009, **44**: 4455.

[9] Cheng H, Ma J, Zhao Z, et al. Hydrothermal Synthesis of $PbTiO_3$ from PbO and TiO_2[J]. *J. Mater. Sci. Lett.*, 1996, **15**: 1245.

[10] Keshri S, Daysl V. Structure and Electrical Transport Properties of Nanosized $La_{0.67}Ca_{0.33}MnO_3$ Sample Synthesized by a Simple Low-cost Novel Route[J]. *J. phys.*, 2008, **70**: 697.

[11] Rao C N R, Mahesh R, Raychaudhuri A K, et al. Giant Magnetoresistance, Charge Ordering and Other Novel Properties of Perovskite Manganates[J]. *J. Phys. Chem. Solids*, 1998, **59**: 487.

[12] Yamamoto T A, Tanaka M, Misaka Y, et al. Dependence of the Magnetocaloric Effect in Superparamagnetic Nanocomposites on the Distribution of Magnetic Moment size[J]. *Scripta Mater.*, 2002, **46**: 89.

[13] Wang G, Wang Z D, Zhang L D. Synthesis and Magnetocaloric Effect of ($La_{0.47}Gd_{0.2}$) $Sr_{0.33}MnO_3$ Polycrystalline Nanoparticles[J]. *Mater. Sci. Eng.*, 2005, B**116**: 183.

[14] Malic. Homogeneity of Pb(Zr, Ti)O-3 Thin Films by Chemical Solution Deposition: Extended X-ray Absorption Fine Structure Spectroscopy Study of Zirconium Local Environment[J]. *J. Appl. Phys.*, 2006, **100**(5): 51612.

[15] Martin-Arbella. Photoactivation of Sol-Gel Precursors for the Low-Temperature Preparation of $PbTiO_3$ Ferroelectric Thin Films[J]. *J. Am. Ceram. Soc.*, 2011, **94**(2): 396.

[16] Schwartz. Chemical Solution Deposition of Electronic Oxide Films[J]. *Comptes Rendus Chimie.*, 2004, **7**(5): 433.

[17] Bretos. Heterostructure and Compositional Depth Profile of Low-temperature Processed Lead Titanate-based Ferroelectric Thin Films Prepared by Photochemical Solution Deposition[J]. *Chem. Mater.*, 2008, **20**(4): 1443.

[18] Zhou H, Hu C H, Yuan J J, et al. Technology of Preparing High-purity Anhydrous Magnesium Chloride by Glycol-ammonia Method[J]. *J. Salt Chem. Industry*, 2007, **167**: 6850.

[19] Maneesha G, Poonam Y, Wasi K, et al. Low Temperature Synthesis and Magneto Resistance Study of Nano $La_{1-x}Sr_xMnO_3$ (x = 0.3, 0.33, and 0.4) Perovskites[J]. *Adv. Mat. Lett.*, 2012, **3**(3): 220.

[20] Mendelson M I. Average Grain Size in Polycrystalline Ceramics[J]. *J. Am. Ceram. Soc.*, 1969, **52**: 443.

[21] Jin A J, Kyunghwan P, Dong H L, et al. The Characteristics of YAG: Ce Phosphor Powder Prepared Using via NO_3-Malonic Acid-NH_4NO_3-$NH_3 \cdot H_2O$ System[J]. *Bull. Korean Chem. Soc.*, 2012, **33**(4): 1141.

[22] Evetts J E, Mathur N D, Isaac S P, et al. Defect Induced Spin Disorder and Magnetoresistance in Single-crystal and Polycrystal Rare-earth Manganite Thin Flms[J]. *Philos. Trans. R. Soc. Lond: Ser. A*, 1998, **356**: 15.